Conclusions

An experimental investigation of the RR→MR and MR→RR transitions over concave and convex, smooth and rough wedges revealed that 1) as the surface roughness increases, the wedge angle at which transition takes place (for a given Mach number) decreases and 2) for a mesh 40 sand paper type surface roughness, it seems that the transition angle becomes independent of the incident shock wave Mach number, i.e., a) MR→RR transition occurs at $\theta_w \simeq 54$ deg and b) RR→MR transition takes place at $\theta_w \simeq 27$ deg.

These results should be of great importance to those dealing with reflections of blast waves, since this type of problem involves nonstationary flows and high degrees of surface (ground) roughness.

Acknowledgments

The authors would like to express their appreciation to Prof. M. Honda of the Institute of High Speed Mechanics, Tohoku University, Japan for his encouragement throughout the present study. The authors are indebted to Mr. O. Onodera for his help in conducting the present experiments.

References

[1] Ben-Dor, G. and Glass, I. I., "Domains and Boundaries of Nonstationary Oblique Shock Wave Reflexions: 1. Diatomic Gas," *Journal of Fluid Mechanics*, Vol. 92, Pt. 3, June 1979, pp. 459-496.

[2] Ben-Dor, G. and Glass, I. I., "Domains and Boundaries of Nonstationary Oblique Shock Wave Reflexions: 2. Monatomic Gas," *Journal of Fluid Mechanics*, Vol. 96, Pt. 4, Feb. 1980, pp. 735-756.

[3] Ben-Dor, G., "Steady Oblique Shock Wave Reflections in Perfect and Imperfect Monatomic and Diatomic Gases," *AIAA Journal*, Vol. 18, Sept. 1980, pp. 1143-1145.

[4] Ben-Dor, G., Takayama, K., and Kawauchi, T., "The Transition from Regular to Mach Reflection and from Mach to Regular Reflection in Truly Nonstationary Flows," *Journal of Fluid Mechanics*, Vol. 100, Pt. 1, 1980, pp. 147-160.

[5] Takayama, K., Honda, M., and Onodera, O., "Shock Propagation along 90 Degree Bends," Institute of High Speed Mechanics, Tohoku Univ., Vol. 35, 1977.

[6] Ben-Dor, G., "Regions and Transitions of Nonstationary Oblique Shock-Wave Diffractions in Perfect and Imperfect Gases," UTIAS Rept. 232, Aug. 1978.

[7] Takayama, K. and Kawauchi, T., "Shock Diffraction over Concave and Convex Walls," Institute of High Speed Mechanics, Tohoku Univ., Vol. 44, No. 391, 1980.

AIAA 81-4229

Transonic Dip Mechanism of Flutter of a Sweptback Wing: Part II

Koji Isogai*
National Aerospace Laboratory, Tokyo, Japan

IT is well known that a sweptback wing experiences a sharp drop of the flutter boundary in the transonic regime, called the transonic dip phenomenon. A possible mechanism of the phenomenon is presented in Ref. 1. The main conclusion reached in Ref. 1 was that the large time lag between the aerodynamic pressures and the airfoil motion, which is due to the compressibility effect, in the transonic region produces a large negative damping for the first bending mode of a sweptback wing and, thus, the mechanism of a single-degree-of-freedom flutter is dominating at the bottom of the transonic dip when the mass ratio is relatively large. This conclusion was derived from the flutter analysis of a two-dimensional wing having vibrational characteristics similar to a typical streamwise section of a sweptback wing. However, since the unsteady aerodynamic forces employed for the flutter analysis were those predicted by linear subsonic theory,[2] important nonlinear aerodynamic effects such as a shock wave were not taken into account. As pointed out by Ashley,[3] the role of the shock in the transonic flutter of a wing must be of great importance. In view of this, a computer code[4] has been developed to solve the transonic small perturbation (TSP) equation numerically by a finite-difference method. This TSP code can be applied for a wide range of reduced frequency, based on semichord, of $0 \lesssim k \lesssim 0.50$ at transonic Mach numbers from subcritical to above Mach 1. The finite-difference scheme employed in the code is a time-marching semi-implicit and implicit two-sweep procedure. To capture the shock wave, a quasiconservative scheme is employed. Further details of the scheme and the validation of the code are outlined in Ref. 4. The purpose of this Note is to recalculate the flutter boundary of the same binary (bending-torsion) system treated in Ref. 1, this time using the nonlinear aerodynamic forces predicted by the TSP code, and to identify the role of a shock wave in the transonic dip phenomenon.

The airfoil considered is a NACA 64A010 (at zero mean angle of attack). In Fig. 1, the mean steady pressure distributions on the airfoil are shown for Mach numbers 0.70, 0.75, 0.775, 0.80, 0.825, 0.85, 0.875, 0.90, and 1.01. In the figure, P and P_0 are the static and stagnation pressures, respectively, and $(P/P_0)^*$ indicates the sonic condition. The flutter boundaries corresponding to these Mach numbers are determined by employing the conventional U-g method. Further details of the present flutter analysis can be found in Ref. 4. The natural vibration modes and frequencies (ω_1 and ω_2) of the binary system used in the present flutter analysis are shown in Fig. 2, where ω_α is the uncoupled frequency in pitch. As pointed out in Ref. 1, the existence of the pivotal point ahead of the leading edge in the first natural mode is one of the key factors in the mechanism of the transonic dip. The x coordinate of the pivotal point x_{pv} (percent semichord, minus toward the leading edge) is -3.87 for the first natural mode and -0.13 for the second. The calculated flutter velocity coefficients $U_F/(b\omega_\alpha\sqrt{\mu})$ (where U_F is the flutter velocity, b the semichord, and μ the mass ratio) for $\mu = 60$ are also plotted in Fig. 2 as a function of Mach number and compared with those predicted by the linear aerodynamic theory [doublet-lattice method (DLM)[2]]. (At $M_\infty = 0.875$, the periodic solution of the unsteady aerodynamic forces has not been obtained, although the solution is numerically stable. Therefore, the flutter points at $M_\infty = 0.85$ and 0.90 are connected by the dotted line.) As seen in Fig. 2, a sharp transonic dip of the flutter boundary is predicted when the nonlinear aerodynamic forces (TSP code) are used. (The exact agreement of the TSP results with those of the DLM at $M_\infty = 0.70$ seems to be fortuitous since there still exists some effect of the airfoil thickness in the aerodynamic forces even for $M_\infty \lesssim 0.70$.) When looking at the mean steady-pressure distributions shown in Fig. 1 and the sonic line and shock-wave patterns shown in Fig. 2, it is noted that the behavior of the shock wave vs Mach number has a close relation with the behavior of the flutter boundary. (The vertical scale of the sonic line pattern at $M_\infty = 0.90$ is reduced somewhat for illustration purposes.) At Mach numbers 0.825 and 0.85, when the flutter speed takes a minimum value, the shock wave is located at 60% chord position at $M_\infty = 0.825$ and 75% chord position at $M_\infty = 0.85$, respectively, on the airfoil. However, at $M_\infty = 0.90$, when the flutter speed increases abruptly to a value six times that at $M_\infty = 0.825$ and 0.85, the

Received Sept. 26, 1980; revision received March 19, 1981.

*Senior Researcher. Member AIAA.

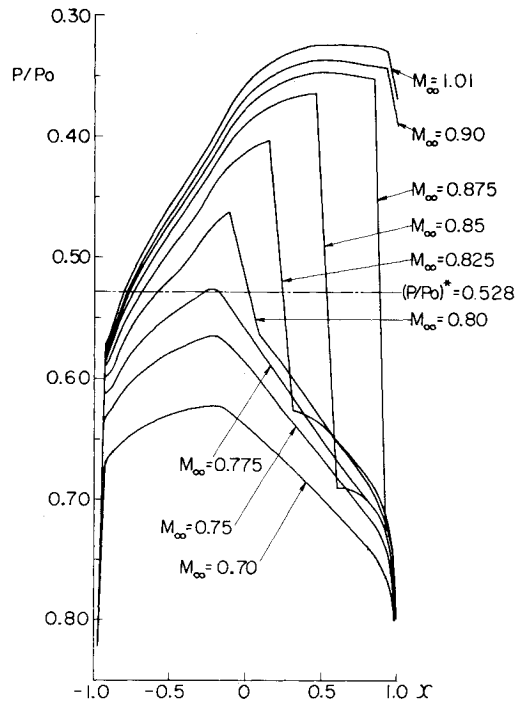

Fig. 1 Mean steady-pressure distributions on NACA 64A010 airfoil at zero mean angle of attack.

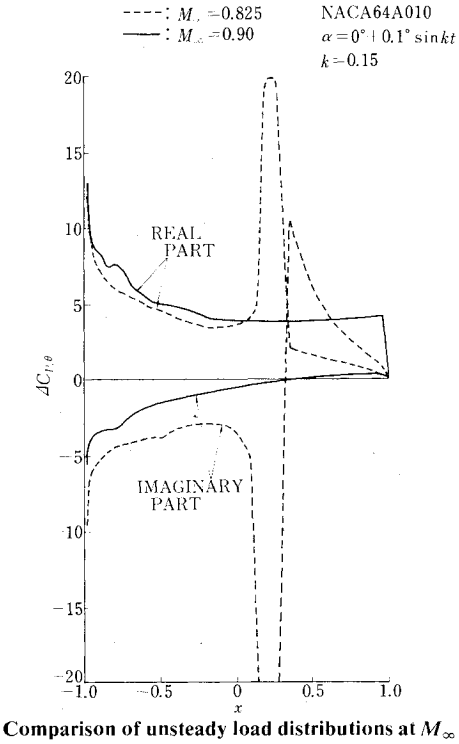

Fig. 3 Comparison of unsteady load distributions at $M_\infty = 0.825$ and 0.90 for NACA 64A010 airfoil oscillating in pitch about midchord axis.

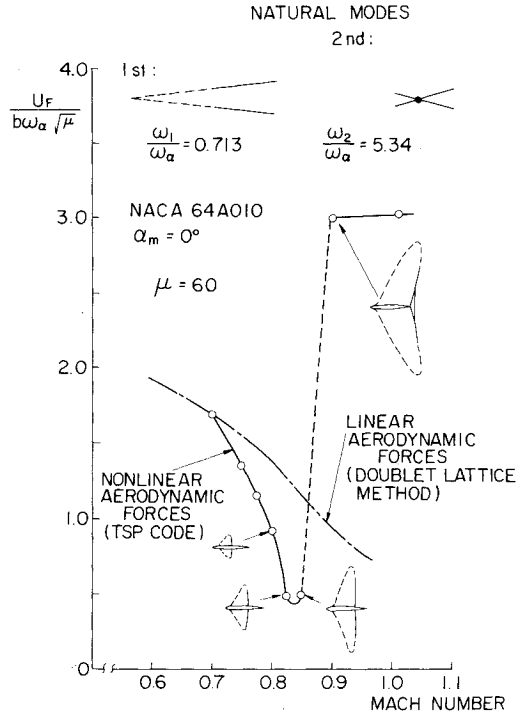

Fig. 2 Natural vibration modes and flutter velocity coefficient vs Mach number for NACA 64A010 airfoil at zero mean angle of attack.

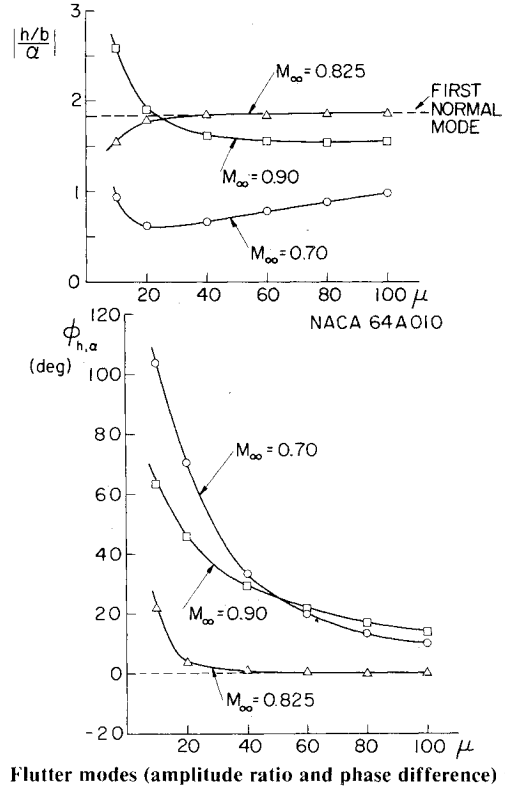

Fig. 4 Flutter modes (amplitude ratio and phase difference) vs mass ratio.

shock wave is located at the trailing edge. Such differences of the mean steady-shock patterns are well reflected in the unsteady load distributions. In Fig. 3, the unsteady load distributions (the first harmonics) at $M_\infty = 0.825$ and 0.90 are plotted in the same figure to contrast the effect of the shock wave. At $M_\infty = 0.825$ there is a sharp peak value at about 60% chord position, especially in the out-of-phase component, while at $M_\infty = 0.90$ there is no such peak value in both the in-phase and out-of-phase components because the shock is already at the trailing edge. This is especially important when we consider the possible cause of the large difference of the flutter speeds between the two Mach numbers. It can be easily confirmed that the large negative value of the out-of-phase component produces large negative damping for the first natural mode of this system, for which the pivotal point is located about 1.5 chord ($x_{pv} = -3.87$) upstream of the leading edge. Thus, the large negative peak value of the out-of-phase component at 60% chord position for $M_\infty = 0.825$ enables the occurrence of a single-degree-of-freedom flutter whose mode is almost identical to the first natural mode. This can be confirmed by examining the flutter mode shown in Fig. 4, where the amplitude ratio ($|(h/b)/\alpha|$) and phase difference

($\phi_{h,\alpha}$) between the plunging and pitching motions at the elastic axis vs mass ratio are plotted for three typical Mach numbers. At $M_\infty = 0.825$, the phase difference rapidly decreases to zero with increasing mass ratio, while the amplitude ratio approaches to the constant value of 1.86 when μ is greater than 40. Since the zero phase difference between the plunging and pitching motions implies the existence of the pivotal point at $x_{pv} = a - (h/b)/\alpha$ (a is the elastic axis position behind midchord in percent semichord and $a = -2.0$ for the present system), the flutter mode at $M_\infty = 0.825$ for μ greater than 40 is essentially a pitching oscillation with pivotal point at $x_{pv} = -3.86$, which is almost identical to the first natural mode shown in Fig. 2. Therefore, when we recall the fact that the large negative peak value of the out-of-phase component in the load distribution at $M_\infty = 0.825$ is due to the phase lag of the shock wave motion, it is concluded that the shock wave (especially the phase delay of the shock-wave motion) is playing the dominant role in the mechanism of the transonic dip phenomenon.

It is believed that the conclusions reached in this investigation may shed some light on the mechanism of the transonic dip phenomenon of a sweptback wing flutter, although the important viscous and three-dimensional effects are still not taken into account in the present analysis.

References

[1] Isogai, K., "On the Transonic-Dip Mechanism of Flutter of a Sweptback Wing," *AIAA Journal*, Vol. 17, July 1979, pp. 793-795.

[2] Albano, E. and Rodden, W. P., "A Doublet-Lattice Method for Calculating Lift Distributions on Oscillating Surfaces in Subsonic Flows," *AIAA Journal*, Vol. 7, Feb. 1969, pp. 279-285.

[3] Ashley, H., "Role of Shocks in the 'Sub-Transonic' Flutter Phenomenon," *Journal of Aircraft*, Vol. 17, March 1980, pp. 187-197.

[4] Isogai, K., "Numerical Study of Transonic Flutter of a Two-Dimensional Airfoil," National Aerospace Laboratory, Japan, TR-617T, July 1980.

AIAA 81-4230

New Approach to the Solution of Falkner-Skan Equation

A. Aziz*
University of Riyadh, Saudi Arabia
and
T. Y. Na*
University of Michigan-Dearborn, Dearborn, Mich.

Introduction

THE Falkner-Skan equation is a celebrated equation in fluid mechanics. It describes the two-dimensional, incompressible boundary-layer flow over a wedge when the freestream velocity u_∞ is of the form $u_\infty \sim x^{(\beta/2-\beta)}$. In mathematical terms, it constitutes a third-order, nonlinear two-point boundary-value problem and is usually written as

$$f''' + ff'' + \beta[1 - (f')^2] = 0 \tag{1}$$

$$f(0) = f'(0) = 0; \qquad f'(\infty) = 1 \tag{2}$$

Since no closed-form solution is known, a variety of numerical schemes have been used and solutions for a range of values of β tabulated. The standard shooting technique in which a succession of values of $f''(0)$ are guessed until $f'(\infty) = 1$ is satisfied has been used by Smith[1] and Elzy and Sisson.[2] However, a major difficulty arises for negative values of β. For example, with $\beta = -0.19$, three values of $f''(0) = 0.040$, 0.08570, and 0.130 satisfy the condition $f'(\infty) = 1$, of which the physically meaningful solution is the one with $f''(0) = 0.08570$.

In a later study, Cebeci and Keller[3] used Newton's method to refine the initial guess and found that with their scheme, the solution automatically converged to the one that was physically relevant. However, the convergence still depended on the initial guess. To circumvent this difficulty, a further refinement was introduced by employing the parallel shooting method in which the boundary layer was divided into three subintervals. This necessitated guessing of seven values, instead of one, though the sensitivity of the solution to initial guess was reduced significantly. Most recently, Zagustin et al.[4] adopted the quasilinearization scheme to obtain the solution. Being akin to Newton's method, it also has the disadvantage that a poor initial guess leads to divergence.

Other numerical efforts toward solving the Falkner-Skan equation have concentrated on using noniterative schemes such as parameter differentiation,[5,6] general parameter mapping,[7] and invariant imbedding.[6] Based on our own experience with the present problem, all three methods could be regarded comparable in computational effort and accuracy.

In the present work, we describe a new approach to solve the Falkner-Skan equation. Compared to the previously cited methods, the present method is much simpler both in concept and computation but yields results of high accuracy. To solve Eqs. (1) and (2), we first assume a regular perturbation expansion for f as a power series in β and generate a total of eleven terms. As is usual, attention is focused on the quantity $f''(0)$ which is a measure of wall shear. The resulting series for $f''(0)$ is found to converge for small values of β. However, the range of applicability and accuracy are remarkably improved by forming the partial sums and applying the Shanks transformation[8] five times. Indeed, for the entire range of physical interest, that is, $-0.19884 \le \beta \le 2$, the procedure yields values of $f''(0)$ correct to four decimal places for most values of β and to three decimal places for others, when compared to the solutions of Smith[1] and Cebeci and Keller.[3]

Solution Method

Considering Eqs. (1) and (2), we assume a regular perturbation expansion in β of the form

$$f = \sum_{n=0}^{\infty} \beta^n f_n \tag{3}$$

Substituting Eq. (3) into Eqs. (1) and (2), equating like coefficients of β, and truncating the expansion at the eleventh term, we have

$$\beta^0 : f_0''' + f_0 f_0'' = 0 \tag{4}$$

$$f_0(0) = f_0'(0) = 0; f_0'(\infty) = 1 \tag{5}$$

$$\beta^n : f_n''' + f_0 f_n'' + f_0'' f_n = \phi_n \tag{6}$$

$$f_n(0) = f_n'(0) = 0; f_n'(\infty) = 0 \quad (n = 1,2,\ldots,10) \tag{7}$$

where ϕ_n for successive terms in the series are

$$\phi_1 = (f_0')^2 - 1 \tag{8}$$

$$\phi_2 = 2f_0' f_1' - f_1 f_1'' \tag{9}$$

Received Dec. 4, 1980; revision received March 6, 1981.

*Professor, Department of Mechanical Engineering.